# Wide-field VLBI Imaging

M.A. Garrett <sup>a</sup> R.W. Porcas <sup>b</sup> A. Pedlar <sup>c</sup> T.W.B. Muxlow <sup>c</sup> S.T. Garrington <sup>c</sup>

<sup>a</sup> Joint Institute for VLBI in Europe, Postbus 2, 7990 AA Dwingeloo, The Netherlands

<sup>b</sup> Max-Planck-Institut für Radioastronomie, Auf dem Hügel 69, Bonn 53121, Germany

<sup>c</sup>NRAL, Jodrell Bank, Macclesfield, Cheshire, SK11 9DL, UK

#### Abstract

We discuss the technique of Wide-field imaging as it applies to Very Long Baseline Interferometry (VLBI). In the past VLBI data sets were usually averaged so severely that the field-of-view was typically restricted to regions extending a few hundred milliarcseconds from the phase centre of the field. Recent advances in data analysis techniques, together with increasing data storage capabilities, and enhanced computer processing power, now permit VLBI images to be made whose angular size represents a significant fraction of an individual antenna's primary beam. This technique has recently been successfully applied to several large separation gravitational lens systems, compact Supernova Remnants in the starburst galaxy M82, and two faint radio sources located within the same VLA FIRST field. It seems likely that other VLBI observing programmes might benefit from this wide-field approach to VLBI data analysis.

With the raw sensitivity of global VLBI set to improve by a factor 4-5 over the coming few years, the number of sources that can be detected in a given field will rise considerably. In addition, a continued progression in VLBI's ability to image relatively faint and extended low brightness temperature features (such as hotspots in large-scale astrophysical jets) is also to be expected. As VLBI sensitivity approaches the  $\mu$ Jy level, a wide-field approach to data analysis becomes inevitable.

Key words: techniques: interferometric, image processing,, methods: data analysis PACS: 95.75.-z, 95.75.Mn, 98.58.Mj

## 1 Introduction

The undistorted field of view of a given VLBI data set is usually limited by two main effects: bandwidth smearing and time-average smearing (Bridle & Schwab, 1989). The narrower the individual frequency channels and the smaller the integration time, the larger the unaberrated field of view. Data generated by VLBI correlators are comprised of a set of measurements of the complex visibility as a function of frequency (or delay) and time. Most continuum VLBI data sets are delivered to the astronomer with relatively narrow frequency channels ( $\sim 0.5 \text{ MHz}$ ) and short integration times ( $\sim 2 \text{ secs}$ ). For example, a typical  $\lambda 18 \text{ cm}$  EVN data set, in its original form, boasts a field-of-view,  $\theta_{fov}$ , in excess of  $\sim \frac{1}{2}$  arcminute. The same EVN data set, having for example being averaged in frequency over  $\sim 64 \text{ MHz}$ , has a field-of-view of  $\sim 300 \text{ milliarcseconds}$  (mas). This reduction in the field-of-view by a factor in excess of two orders of magnitude is often considered to be unimportant. The aim of this paper is to show, by illustration, that this presumption may no longer be valid.

# 2 New Developments in Wide-Field VLBI Imaging

In the early 1980s, the off-line computer resources available to most astronomers were ill-equipped to deal with extremely large and cumbersome VLBI data sets. Not surprisingly, one of the major goals of VLBI data reduction was to severely average continuum data at the earliest possible stage in the analysis process (as soon as fringe-fitting corrections had been applied). Today, the processing power and data storage volumes enjoyed by the vast majority of VLBI astronomers is  $\sim 2$  orders of magnitude greater than the shared systems used previously. Nevertheless, the custom of excessive data averaging continues. This practice severely limits the natural field of view of VLBI images, and is often inappropriate - especially in the era of high sensitivity observations.

#### 2.1 Detection of hot-spots in Large-scale Jets

In Fig. 1 we present a  $\lambda=18$  cm EVN-only map of the gravitational lens, 0957+561 A,B. The data were calibrated in the usual manner. To avoid bandwidth smearing, the data were held in the form of 28 independent but contiguous 2 MHz channels. The data were averaged in time in a baseline dependent manner with integration times ranging from 2.5 seconds (on the longest projected baselines) to 30 seconds (on the shortest projected baselines). Fig. 1 clearly shows the two main, compact components, 0957+561 A,B and a very

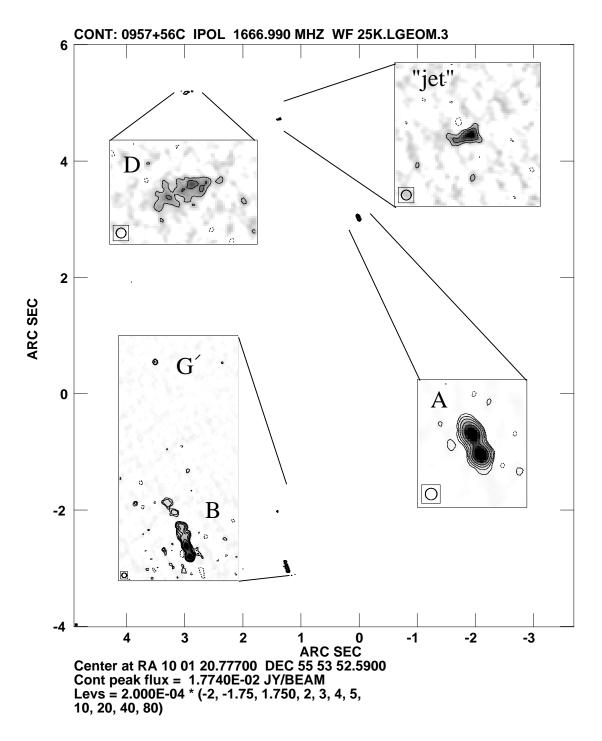


Fig. 1. A wide-field image of the gravitational lens system 0957+561. In addition, to the previously known compact features (A,B, G') we also detect compact structure in the arcsec-scale jet (previously labelled in VLA maps of the source as features "jet" and "C".

faint compact source known as G', lying about 1 arcsec to the north of B. All three components have been detected by previous VLBI campaigns. However, the real excitement relates to the fact that we have detected and imaged

two low brightness temperature features ( $T_b \sim 10^6 - 10^7$  K), that are associated with compact regions or hot-spots in the singly imaged arc-second scale jet that dominates VLA maps of this source. There must be many more cases where similar low surface brightness emission goes undetected, simply because a wide-field approach to the data analysis is not pursued. VLBI observations of such emission could improve our understanding of large-scale jet physics, distinguishing between various hot-spot models and allowing a comparison between the properties of the jet (e.g. flow velocity) and the intergalactic medium on pc and kpc scales.

## 2.2 Imaging Faint SNR in the Starburst Galaxy M82

A wide-field approach has also been applied by Pedlar et al. (1999) to  $\lambda 18$  cm EVN observations of the starburst galaxy M82. Previous VLBI observations had focussed on the brightest SNR (41.95+575), but by following a wide-field approach to the data analysis Pedlar et al. (1999) have been able to generate exquisite images of 4 other compact SNR in the field, of which the faintest has a peak flux of  $\sim 0.4$  mJy/beam. A sub-section of the entire 1 arcminute field is shown in Fig. 2. Pedlar et al. (1999) have also re-analysed "vintage" EVN data of M82 from epoch 1986. By employing a wide-field approach to the re-analysis they have been able to measure expansion rates for one of the SNR and place upper-limits on two others. This work is a superb example of the type of information "gain" one can easily acquire through the general application of wide-field techniques to VLBI data.

# 2.3 Going Deeper into a Crowded Sky

The advances in VLBI hardware described elsewhere in this volume suggest that for a Global VLBI array r.m.s. noise levels of  $\sim 10~\mu \rm{Jy/beam}$  will be attainable by the end of the millennium. Looking further ahead (10-15 years) there is every reason to believe that  $\sim 1~\mu \rm{Jy/beam}$  noise levels will be achievable. At this level of sensitivity, the radio sky becomes a very crowded place. At the  $\mu \rm{Jy}$  level one may expect to encounter 1 source every few arcseconds (see Muxlow et al. (1999)). We can expect to reach these levels of sensitivity within the next 10-20 years, by which time wide-field VLBI imaging may have evolved into a standard VLBI processing route in order to avoid source confusion. Even at the level of a few mJy a wide-field approach may pay dividends. Garrington et al. (1999) have embarked on a survey of faint mJy sources located within a few degrees of a bright, compact radio source, 1156+295. Two of the faint sources surveyed are separated by only a few arcminutes on the sky. Even although the observations had not been set up with wide-field imag-

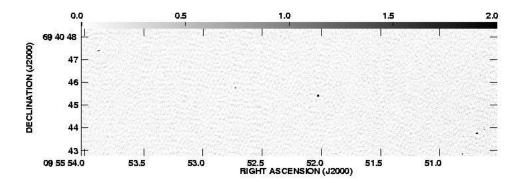


Fig. 2. A large wide-field image of part of the M82 field imaged by Pedlar et al. (1999). Four supernovae are clearly detected in this image, only the brightest (bottom right hand corner) was detected by previous VLBI observations.

ing specifically in mind, it was still possible to produce tapered images of both sources simultaneously from a single  $\lambda 6$  cm global VLBI data set (see Fig. 3). We note that this wide-field approach permits a very *direct* measurement of the relative astrometric positions of radio sources in the same undistorted field of view.

# 3 Current Limitations

Currently the main limits on wide-field imaging are set by the maximum data rate that can be generated by VLBI correlators. In other words, the limitation is exactly the reverse of the situation in the early 1980's, where the bottleneck was associated with off-line data processing facilities. Another restriction is the size of the primary beam of the larger VLBI antennas, especially phased arrays (e.g. WSRT & VLA<sub>27</sub>). In this case at least, "small is beautiful". This latter point should be borne in mind when the next generation of large telescope arrays are being designed (e.g. SKA), especially with regard to their possible incorporation within existing VLBI networks.

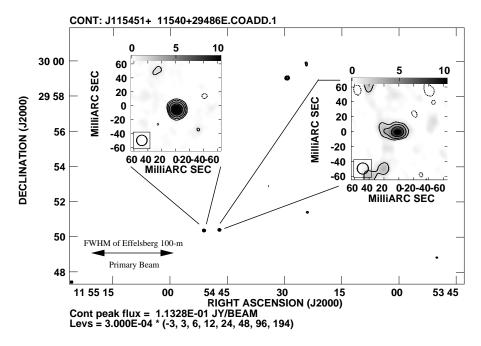


Fig. 3. Global  $\lambda 6$  cm VLBI maps of two closely separated VLA FIRST radio sources generated simultaneously using wide-field data analysis techniques. Both sources are members of a faint source survey (see Garrington et al. (1999)). The total number of sources in this VLA FIRST field gives a good impression of how often one can encounter secondary sources at the mJy level. As VLBI sensitivity approaches the  $\mu$ Jy level, a wide-field approach to data analysis is inevitable.

## References

Bridle, A.H. & Schwab, F.R., 1989, in: Perley, R.A., Schwab, F.R., & Bridle, A.H. (eds), Synthesis Imaging in Astronomy, A.S.P. Conference Series, 6, p 247.

Garrington, S.T., Garrett, M.A., & Polatidis, A., 1999, NewAR, XX, pp. These proceedings.

Muxlow, T.W.B., Wilkinson, P.N., Richards, A.M.S., Kellerman, K.I., Richards, E.A., & Garrett, M.A., 1999, NewAR, XX, pp. These proceedings. Pedlar, A., Muxlow, T.W.B., Garrett, M.A., Diamond, P., Wills, K.A., Wilkinson, P.N., & Alef, W., 1999, NewAR, XX, pp. These proceedings.